DESIGN OF COMPOSITE COMPRESSION MOLDING TOOLS USING LARGE SCALE ADDITIVE MANUFACTURING

Michael Bogdanor[a], Himal Agrawal[a], Eduardo Barocio[a], Anthony Favaloro[a], Brian Smiddy[b], Ken Susnjara[b], R. Byron Pipes[a]
[a]Composites Manufacturing and Simulation Center, Purdue University
West Lafayette, IN, USA
[b]Thermwood Corporation
Dale, IN, USA

ABSTRACT

In this work, both pieces of a two-sided, compression molding tool are additively manufactured and post-processed using Thermwood's Large Scale Additive Manufacturing system. The printed geometries are machined to achieve net shape and for the insertion of cartridge heaters. The matched tools, made from 25% carbon fiber reinforced PESU, are used in the successful compression molding of a demonstration blocker door part made from a thermosetting prepreg platelet molding compound (PPMC). Design of the molded part and the additive manufactured tool was performed using the ADDITIVE3D and PPMC integrated workflow applications, respectively, to determine the manufacturing informed performance of the part and tool. Additionally, heat transfer simulations were performed to inform the molding process and requisite environmental conditions for successful molding including cartridge heater and platen temperature.

Corresponding author: Michael Bogdanor bogdanor@purdue.edu

1. INTRODUCTION

Large scale tooling is emerging as one of the most promising applications of the products of Extrusion Deposition Additive Manufacturing (EDAM). Single sided tools and fixtures for in- and out-of-autoclave composite manufacturing have seen significant development in recent years. Two-sided compression molding introduces several additional challenges beyond those seen in single-sided applications, but as will be discussed herein, modeling and simulation are excellent tools for addressing these challenges. Typical implementation of the EDAM process involves a gantry mounted extruder that deposits a fiber-filled thermoplastic bead onto a build plate. The combined motion of the gantry system and the build plate results in at least three axes of movement yielding parts with dimensions on the order of meters. Current commercial equipment is capable of depositing material at rates more than 500 lbs/hr or 225 kg/hr, typically using carbon fiber-filled, high performance polymers. Unsuccessful prints with large build volumes and high-grade materials result in significant waste in material, time, and cost. As such, there is a tremendous need to be able to predict the outcome of EDAM prints before any material is deposited to reduce the number of physical iterations and replace them with virtual design and optimization iterations. In this case study, the integrated workflow application, ADDITIVE3D, developed at Purdue

University in the Composites Manufacturing and Simulation Center (CMSC), will be exercised to demonstrate the design, modeling, and simulation of a two-sided EDAM tool, printed by Thermwood using the Large Scale Additive Manufacturing (LSAM) machine, for the compression molding of an aerospace blocker door manufactured with a prepreg platelet molding compound (PPMC) and designed using the PPMC3D application.

The EDAM process with fiber-reinforced polymers has enabled the application of additively manufactured (AM) tooling for traditional composite manufacturing processes that include hand layup [1], Vacuum Assisted Resin Transfer Molding (VARTM) [2,3], autoclave curing [4,5], and compression molding [5]. The relative small deformation reported for tools used in VARTM [2] and autoclave [4,5] processes indicates that the thermal stability of the printed composite materials is adequate for prototype tooling. The concept of AM tooling have been adopted in other fields, for instance, patterns for forming sand cavities used in foundries have been produced using the fused filament fabrication process [6], and inserts for injection molding have been produced with PolyJet® process [7].

EDAM tooling offers several benefits in composites manufacturing and prototyping efforts. First, EDAM tooling is generally lighter and more rapid to produce than the metal counterpart. Furthermore, AM can produce geometries for tooling that are not possible in subtractive manufacturing and can be utilized to place internal cavities and cutouts in large structures. The technology also offers the possibility of tailoring the printing path to match the coefficient of thermal expansion (CTE) of the part to be molded with the tool, this is particularly beneficial in molding of composite parts which themselves exhibit high degrees of anisotropy to minimize part deformation off the tool.

Modeling and simulation are key drivers in understanding the printing process and the performance of EDAM products. The previously developed ADDITIVE3D workflow [8–11] simulates the entire printing process using a time-dependent, coupled thermo-mechanical analysis that directly models the polymer kinetics, temperature dependent heat transfer behavior, and resulting viscoelastic mechanical behavior. The ADDITIVE3D toolkit includes model initialization based upon the actual machine path. The results can also be mapped to final, as-machined meshes for performance analyses as is the use case herein. The simulations are utilized to study the effects of the print direction on the deformations and interlayer stresses in the resulting part and to assist the designer in optimizing the heating and processing strategy for the part manufacturing process using the printed tools.

In the following sections, a brief overview of the ADDITIVE3D simulation approach is provided first. Next, the details of the case study of the compression molding of a PPMC blocker door using EDAM tooling will be discussed. The following section will describe the modeling and simulation efforts used to design the printed part and the manufacturing process. Then the results of the experimental study and molding trial are presented, demonstrating the successful molding of the part with the EDAM tools. The final section provides the conclusions from the study.

2. TOOLING DESIGN CASE STUDY

The blocker door part (Figure 1a) used in this case study presents a design case of an aerospace part that while not being a flight-critical component, has a design governed by its structural

performance. The blocker door is 300 mm by 200 mm (11.8 in by 7.9 in) with a nominal surface thickness of 4 mm (0.16 in) and ribs up to 30 mm (1.18 in) deep. The ribs were designed with a draft angle of 5 degrees to facilitate demolding. In this representative design, 16 blocker doors are mounted on the outer circumference of the fan duct for a turbofan engine as shown in Figure 1b, shown in the deployed configuration. During typical operation, the blocker doors are stowed along the surface of the fan duct and have a smooth curved surface allowing the air to flow through the duct. When the thrust reversing system is deployed, the blocker doors rotate to restrict the airflow through the bypass and redirect the air through openings on the sides of the fan duct to reduce thrust and slow the aircraft. The blocker door is designed to withstand the pressure load from redirecting the air flow with a stiffness criterion such that the deformation of the geometry does not allow air flow through gaps between adjacent doors. This part is well suited to application of carbon fiber PPMC to meet the strength, stiffness, and weight requirements while maintaining high production rates. Compression molding of the carbon fiber and epoxy PPMC requires heated, two-sided tooling capable of achieving mold surface temperatures of 265 °F (130 °C) and pressure of 1500 psi (10.3 MPa) while maintaining dimensional stability for a 12 to 15-minute curing cycle.

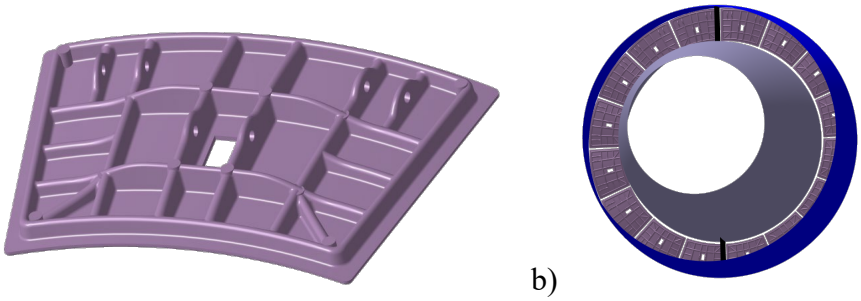

a) b)

Figure 1. Conceptual design for a) composite blocker door and b) blocker door assembly with fan duct.

The two sides of compression molding tool were additively manufactured using Thermwood's LSAM system using a 25wt% CF-PESU from Techmer PM. The efficacy of the compression molding system relies on manufacturing the parts within the required tolerances and the ability of the tool to withstand multiple compression molding cycles for prototype production. Anisotropic thermal expansion of the discontinuous fiber system in conjunction with in-plane printing lead to high anisotropic thermal expansion of the part. These anisotropic thermal expansions need to be accounted for while manufacturing a part to design for geometry change due to local thermal stresses in addition to the local residual stresses from the printing process. Tool shape compensation provides a way to design the shape of the tool to account for anisotropic thermal expansions and hence avoid shape distortion on cooling to maintain final part tolerances.

A common failure observed with additively manufactured tools is the delamination between the printed layers from interlaminar shear and/or tension due to low fracture toughness of the resin system. Hence the tools are typically printed in a way that tensile stress in the through thickness direction is limited to prevent the debonding between layers. In designing for the compression molding process, a tight shear edge is required between the positive and negative tools to ensure that the molding charge stays within the molding cavity. When the two halves of the tool are separated in demolding, significant tensile stress can develop in the tools in the molding direction. Another source of tensile stress that develops is from Poisson effects in the molding

process where high compressive stress in the mold closing direction is accompanied by tensile stresses in the perpendicular directions. Designing for these stresses is critical for successful tooling approaches.

Furthermore, the low thermal conductivity of the printed part perpendicular to local fiber direction leads to high thermal gradients and reduced temperature distribution away from the heat source, be it platens or internal elements. Successful molding requires that the tooling surfaces maintain the resin processing temperature at steady state due to low thermal conductivities of the printed part. Increasing the temperature at the platen surfaces will increase the temperature at the tooling surfaces, but is limited by the glass transition temperature, T_g, of the resin. Two potential solutions to increase the temperature at the molding surface are to place cartridge heaters inside the tool near the molding surface and heat the tool using conduction or creating a heated chamber around the tool and heating the tool using convection. In the design utilized in this demonstration, cartridge heaters are placed inside the tool and the temperature at the platen and at the cartridge heaters is kept below the T_g of the resin to successfully mold PPMC thermoset charge using compression molding. Further, the tool is heated in a closed configuration to simulate some of the effect of having a fully enclosed convection chamber around the tooling surface.

The geometry of the two halves of the tool used for the experiments and simulations is shown in Figure 2, based on the geometry requirements of the blocker door part. The negative tool contains the molding cavity with integrated ribs to provide geometrical stiffness to the resulting part. The molding cavity has a short region of zero draft to create the shear edge between the positive and negative tools and to ensure that the press-closing force is applied to the molding material and not the tool itself. The depth of the zero draft region is based on the size of the charge and part thickness for the blocker door so that the molding material does not escape the cavity during processing. The overall dimensions of the negative tool are 690 mm by 340 mm by 125 mm (27.2 in by 13.4 in by 4.9 in) and the positive tool are 690 mm by 240 mm by 125 mm (27.2 in by 9.4 in by 4.9 in). The tools were designed and manufactured with flanges on the sides to facilitate connection to the platens of the 250-ton compression molding press used at the Indiana Manufacturing Institute (IMI) for the prototype molding trials. Printing and machining of the tools, including installation of the cartridge heater and manufacturing of the heater control system, was performed at Thermwood Corporation in Dale, IN.

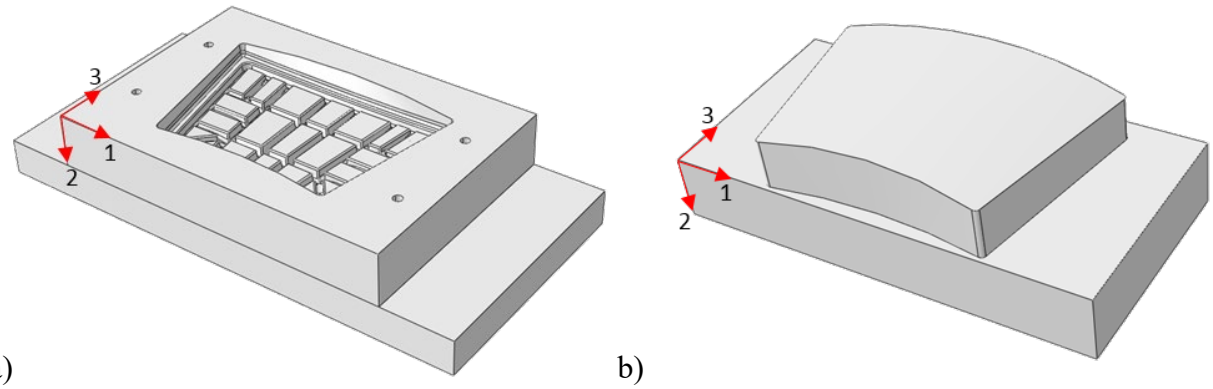

a) b)

Figure 2. Isometric view of the a) negative and b) positive tools.

3. SIMULATION RESULTS

Simulation was used to study the effects of different compression molding conditions and guide the design for AM of the compression molding tool. Characterizing a material for simulating the AM process is intensive and is still ongoing for the 25% CF-PESU. However, a material card for Celanese 50% CF-PPS (polyphenylene sulfide) [12] has been previously validated for the ADDITIVE3D simulation and was used in the study presented herein. There will be significant differences between the material properties of the two materials at the bead level from the difference in fiber loading and polymer kinetics. Thus, the presented simulation results should be considered as providing design guidance (both printing strategy and molding strategy), not quantitative results. Furthermore, as the polymers differ significantly, the effects of the printing process, particularly deformation, will not be well predicted with the current material card. However, the resulting local mechanical properties, thermal expansion, and heat transfer coefficients will be similar. Thus, the process simulation component of ADDITIVE3D was used primarily to map the local material properties of the printed material onto the analysis mesh of the following performance simulations to account for the anisotropic material properties at each integration point in the element as defined by the printing path. Nevertheless, the performed simulations were critical for achieving a successful molding using AM tooling.

Two concerns when designing an AM compression molding tool are the large CTE and the relatively low tensile strength of the printed material in the layer stacking direction (z-direction). While the large CTE is concerning in mold designs that can entrap the molded part upon cooling to room temperature, the low tensile strength is concerning due to stresses introduced in the tool during the process of ejecting the part from the tool. A stress analysis of the ejection process was carried out to study the effect of printing direction in the negative tool and evaluate the performance of the tool against the strength of the interlayer bonds. Figure 3 shows the two printing orientations considered. In either case, the printed geometries are fully-filled and near net shape for the final geometry. A machining step will occur after printing to achieve the final molding surfaces and machine in the molding cavity.

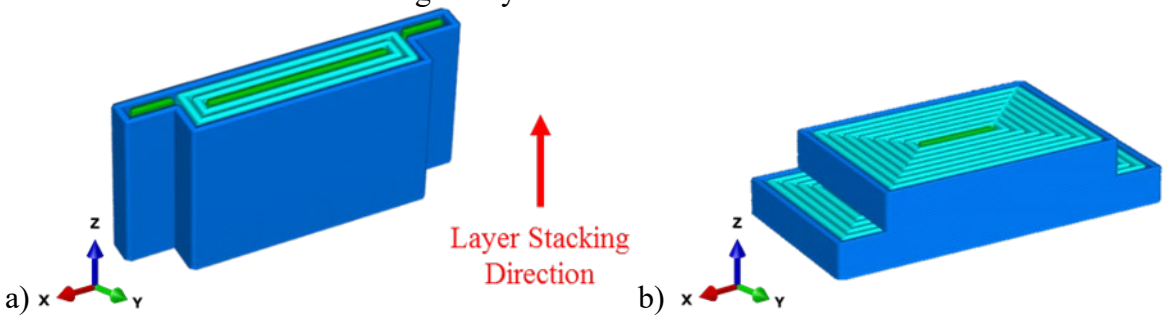

Figure 3. Print paths for the negative tool, oriented a) vertically and b) horizontally.

To simulate the ejection process of the part, the negative tool is clamped in four regions located at the flange of the tool, and a surface traction load was applied in the direction of part ejection. This simulation included effects of manufacturing such as local material orientation and residual stresses after the machining process. Figure 4 shows the stresses in the z-direction resulting from the part ejection process for the two print orientations. Considering a maximum allowable stress in the z-direction of around 30 MPa (4.35 ksi), this study showed that it was less likely to damage the tool during the ejection process if the tool is oriented vertically as shown in Figure 4a.

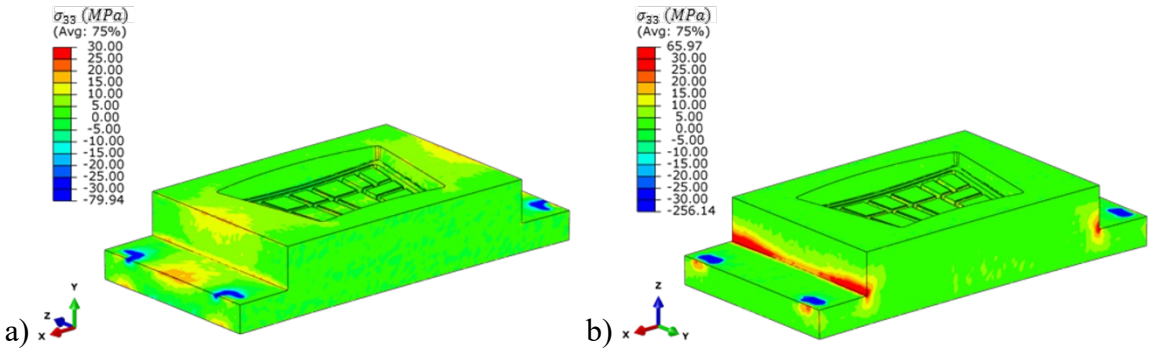

Figure 4. Z-direction normal stress resulting from the part ejection process for tool, oriented a) vertically and b) horizontally.

Prediction of the part behavior under the given molding conditions requires the understanding of the underlying physics behind the heat transfer of the anisotropic printed material. Heat transfer simulations under different thermal conditions were performed to understand and predict the performance of the tools under varying heating strategies. The most important factor for successful molding, beyond maintaining tool surface integrity, is the temperature of the tool at the molding surface which needs to be higher than the processing temperature of the resin for successful compression molding of the part.

Steady state heat transfer simulations were performed with different thermal conditions to find the temperature distribution of the part at the molding surface. Figure 5 shows the side view of the two halves of the tool and the temperature boundary condition at the bottom of the tool surface (marked in red) which is in contact with the platen. All the other surfaces allow natural convection with heat transfer coefficient of 10 W/m-K at an ambient temperature of 27 °C (81 °F).

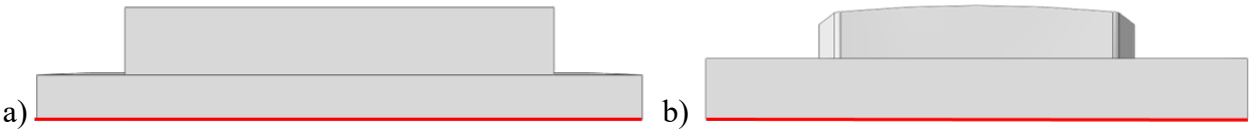

Figure 5. Side view of the a) negative and b) positive tool respectively with red line marking the temperature boundary condition surface.

The temperature applied at the bottom of the tool surface was 212 °C (414 °F), the T_g of the resin, whereas all the other surfaces convect naturally at the ambient temperature of 27 °C (81 °F). The steady state temperature distribution at the molding surface of the negative tool is shown in Figure 6 and that of positive tool in Figure 7.

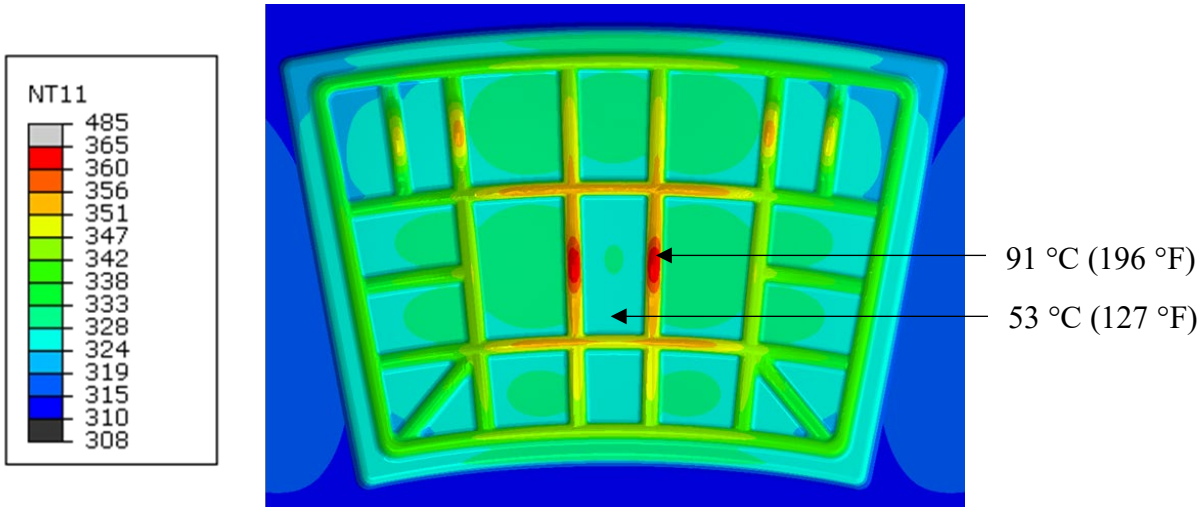

Figure 6. Steady state temperature distribution for negative tool under platen heating alone.

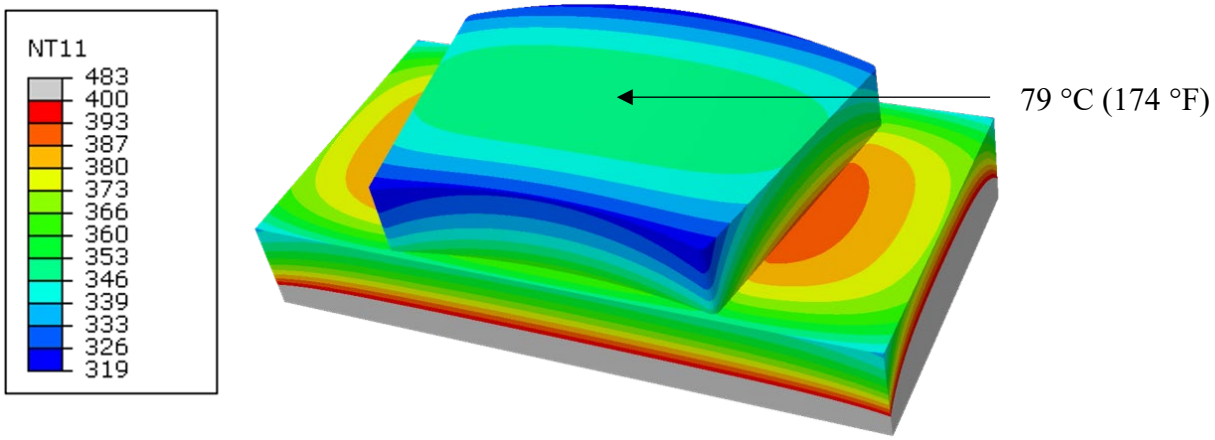

Figure 7. Steady state temperature distribution for positive tool under platen heating alone.

Figure 6 shows the steady state temperature distribution when heating the tool from the platens while the other surfaces convect naturally. The contour plot of the output value, NT11, from the Abaqus heat transfer analysis for surface temperature is reported in Kelvin. The highest temperature recorded in ribs is 91 °C (196 °F) which is less than the 130 °C processing temperature of the resin. A similar observation is made for the positive tool where the average temperature on the molding surface at the center is 77 °C (171 °F) and towards the edges 47 °C (117 °F). Accordingly, it is concluded that platen heating along will be insufficient for heating the tool to the temperatures required for the compression molding process.

Two options for increasing the temperature of the tooling surface are building a heating chamber around the tool and using forced convection or placing a heat source inside the tool and heating the tool using conduction. Both the possibilities have been analyzed with the help of heat transfer simulations using Abaqus. Firstly, the effect of forced convection from a heating chamber on the temperature distribution of the tool has been analyzed. The top surface of the negative and the positive tool have been assigned forced convection boundary conditions with convective heat transfer coefficient h of 20 W/m-K at elevated temperature of 127 °C (261 °F). The boundary

conditions shown in Figure 8 correspond to the practical scenario of building a heating chamber on top of the negative tool and lowering the positive tool into the heating chamber so that the red surface of the positive tool shown is effectively heated through forced convection. The platen is still assigned a temperature boundary condition of 212 °C (414 °F) and the remaining surfaces convect naturally at ambient temperature of 27 °C (81 °F). The steady state temperature distribution is then analyzed for both the halves of the tool.

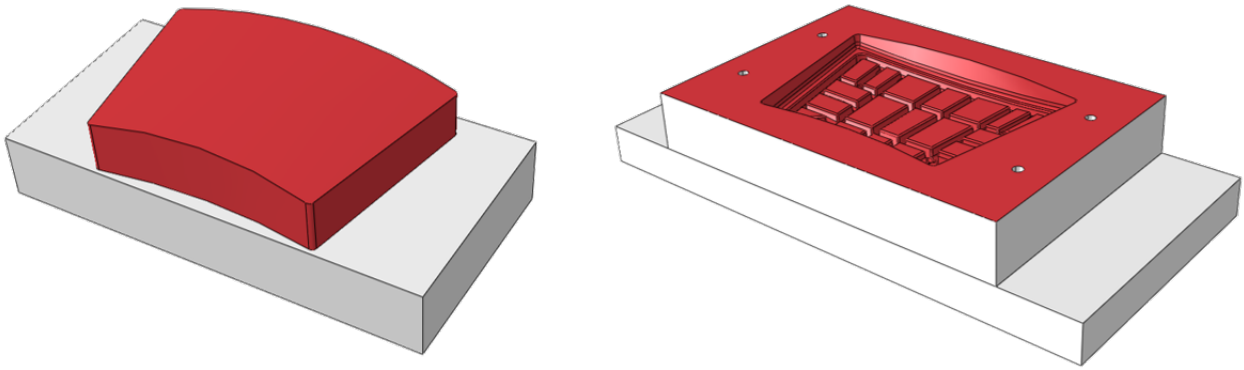

Figure 8. Surfaces assigned forced convection boundary conditions to model heating chamber.

Figure 9 and Figure 10 show the temperature distribution in the negative and the positive tool, respectively. This analysis indicates forced convection at elevated temperatures combined with heating the tool from the platens is expected to provide nearly adequate temperature to support the compression molding process. The average temperature on the molding surface of the negative tool is 127 °C (261 °F) which is close to the processing temperature of the resin with a high of 143 °C (289 °F) at the center ribs of the tool. The temperature distribution in the positive tool ranges from 138 °C (280 °F) at the center to 131 °C (268 °F) at the corners. While the average temperature across the tools is likely to provide enough heat to sufficiently cure the part, the distribution of temperature in the negative tool indicates that there is a potential that the corners of the part will not see sufficient temperature required to locally cure the material.

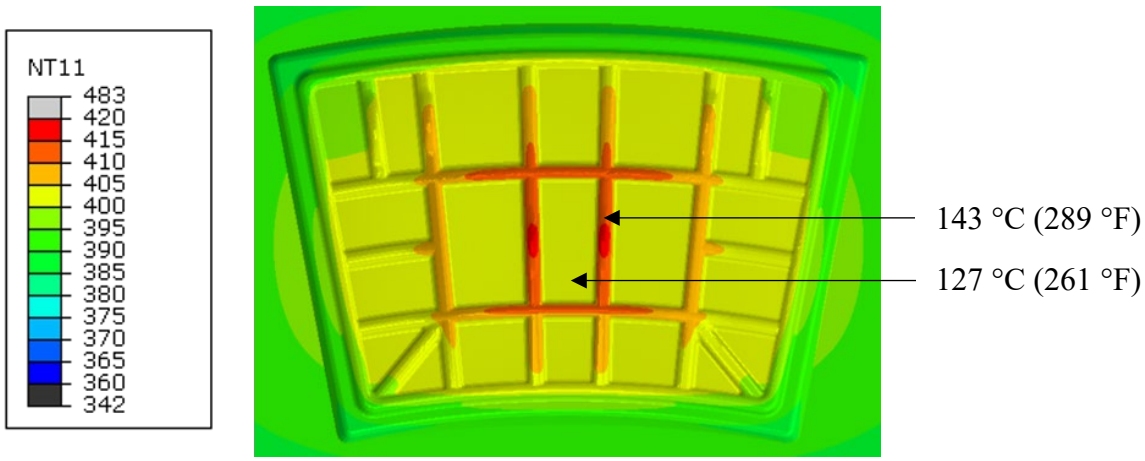

Figure 9. Negative tool steady state temperature distribution for convection combined with platen heating.

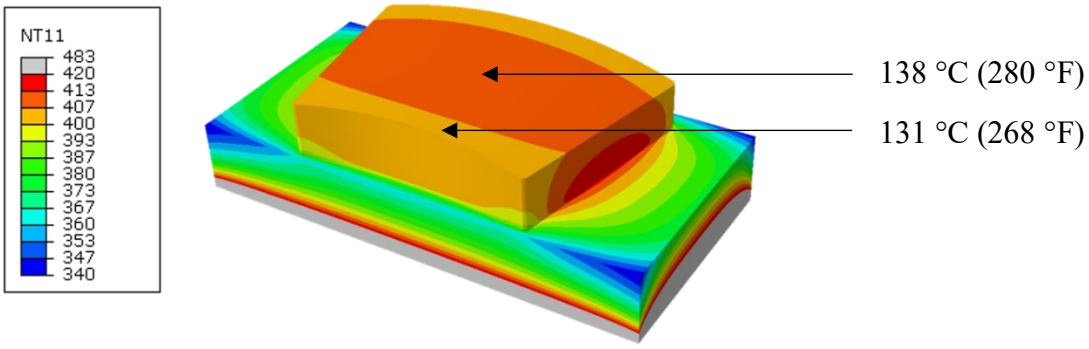

Figure 10. Positive tool steady state temperature distribution for convection combined with platen heating.

One of the challenges with platen heating is the distance that the heat travels from the heat source to the molding surface. Integrated cartridge heaters can be inserted into the tool to reduce this distance that the heat travels. In this study, 1 in (25.4 mm) diameter cartridge heaters were utilized with active controls to regulate the temperature in the heaters to remain below the glass T_g of the PESU. Figure 11 shows the location of cartridge heaters inside the negative and positive tools. Four heaters were inserted through bored holes into the negative tool and three were used in the positive tool. The locations in the negative tool were selected to avoid interference with the ribs in the tooling surface, and the locations in the positive tool were designed to allow the tool to fully close with the heaters engaged.

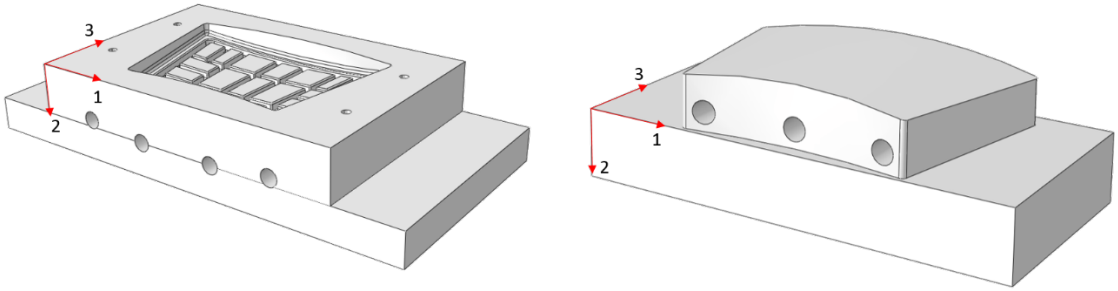

Figure 11. Location of cartridge heaters in the additive manufactured tools.

The temperature of the cartridge heaters was set to 193 °C (379 °F) in the simulations, which is below the T_g of the resin. The steady state temperature distribution is then obtained with the platen at 212 °C (414 °F) and the other surfaces convecting naturally at the ambient temperature of 27 °C (81 °F). Figure 12 and Figure 13 show the temperature distributions at the molding surface of the tool with combined heating from the cartridges and platens. The average temperature at the main surface of the negative tool is 131 °C (268 °F). Some localized regions with temperatures up to 161 °C (322 °F) are present in the ribs where the geometry feature is located close to the cartridge. The temperature distribution over the positive tool is significantly more uniform with the use of the cartridges, with an average temperature of 137 °C (279 °F). The results of the heat transfer analysis indicate that the use of the cartridge heaters is preferred for the compression molding process.

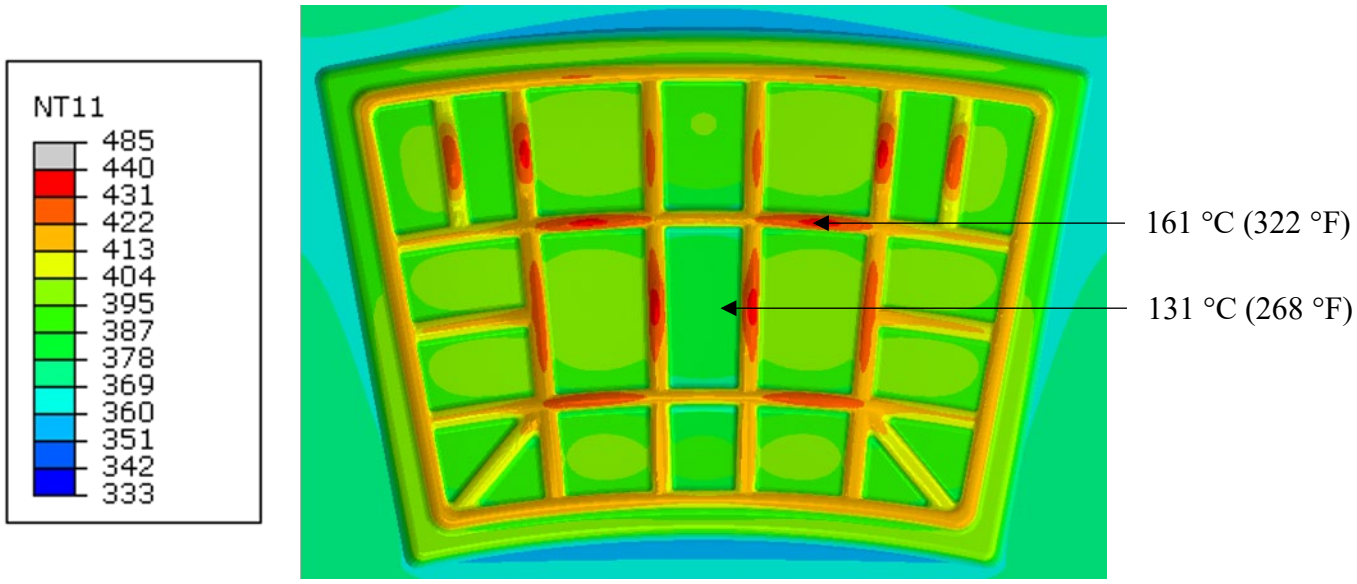

Figure 12. Negative tool steady state temperature distribution for cartridge heating combined with platen heating.

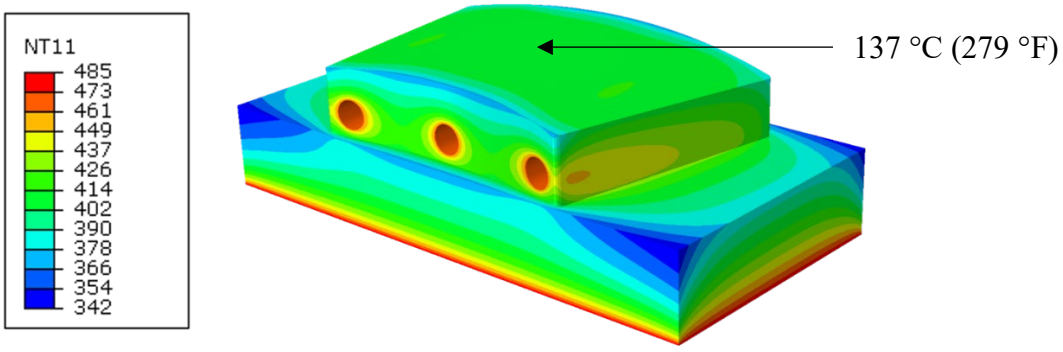

Figure 13. Positive tool steady state temperature distribution for cartridge heating combined with platen heating.

4. EXPERIMENTAL RESULTS

The experimental setup used for compression molding the blocker door part is shown in Figure 14. The seven cartridge heaters were independently controlled from a central unit powered by a 240 V supply. The negative tool was mounted on the lower platen and the positive tool to the upper platen. The printed tools are held in place with metal clamps attached to the side flanges. Two metal plates were affixed to the negative tool on either side and attached to each other with bolts running through the printed tool to provide a pre-compressive stress to the geometry and resist interlaminar tensile stress to maintain tool integrity. Both sides of the tool were pretreated with a mold-release coating. The upper and lower platens of the press were set to temperatures of 205 °C (400 °F) and 210 °C (410 °F), respectively, and the cartridge heaters were set to 193 °C (379 °F).

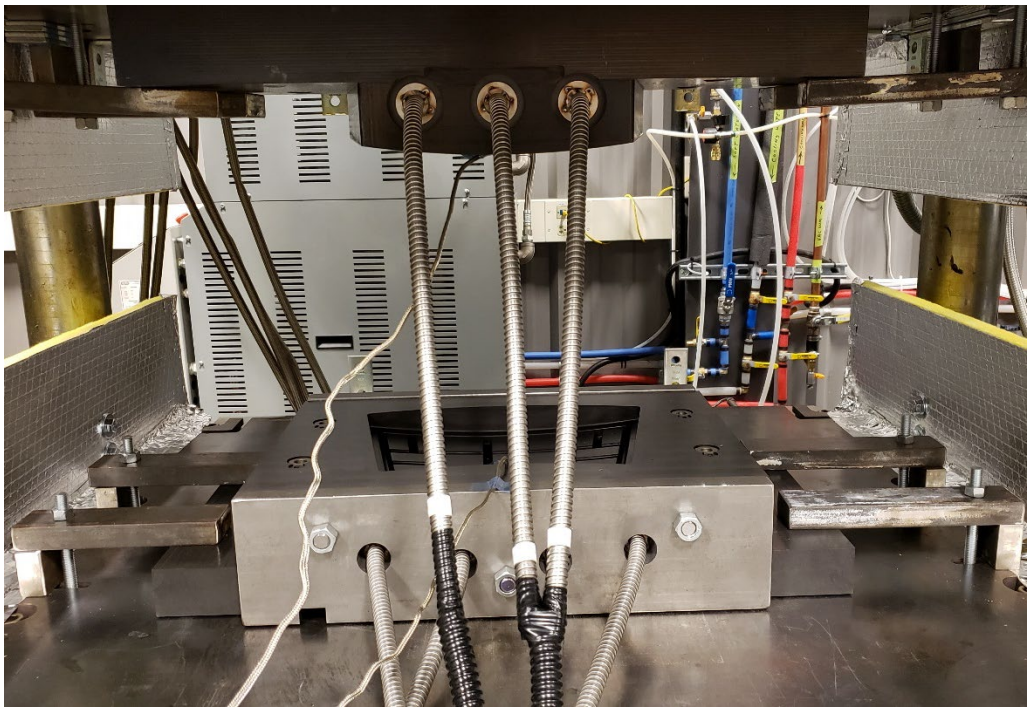

Figure 14. LSAM printed tools with cartridge heaters mounted on the 250-ton compression molding press at the IMI.

The temperature of the molding surface was monitored using an infrared camera and the temperature of the cartridge heaters was adjusted to maintain consistent temperature on the molding surfaces of the positive and negative tools to avoid residual stresses formation due to temperature difference. After the tools were mounted and aligned at room temperature, the system was heated with the two tools in near-contact. The upper and lower platens of the press were set to temperatures of 205 °C (400 °F) and 210 °C (410 °F), respectively, and the cartridge heaters were set to 193 °C (379 °F). Once the set temperatures were achieved, the tool was cycled to ensure the fit between the matched tools.

Prior to placing the molding charge into the negative tool, the temperature distribution was obtained for the positive and negative tool from the infrared camera as shown in Figure 15 and Figure 16 on a Celsius scale. The temperature distribution obtained from the infrared camera for the molding trial closely matches the temperature distribution obtained from the simulation. The surface temperature of the positive tool from infrared camera is in the range of 125 to 130 °C (257 to 266 °F) compared to the predicted average surface temperature from the simulations of 127 °C (261 °F). Similarly for the negative tool, the thermal imaging reveals local temperature increases in the ribs in the range of 160 °C (320 °F) and a temperature on the main surface closer to 130 °C (266 °F) following the trend of the simulation result.

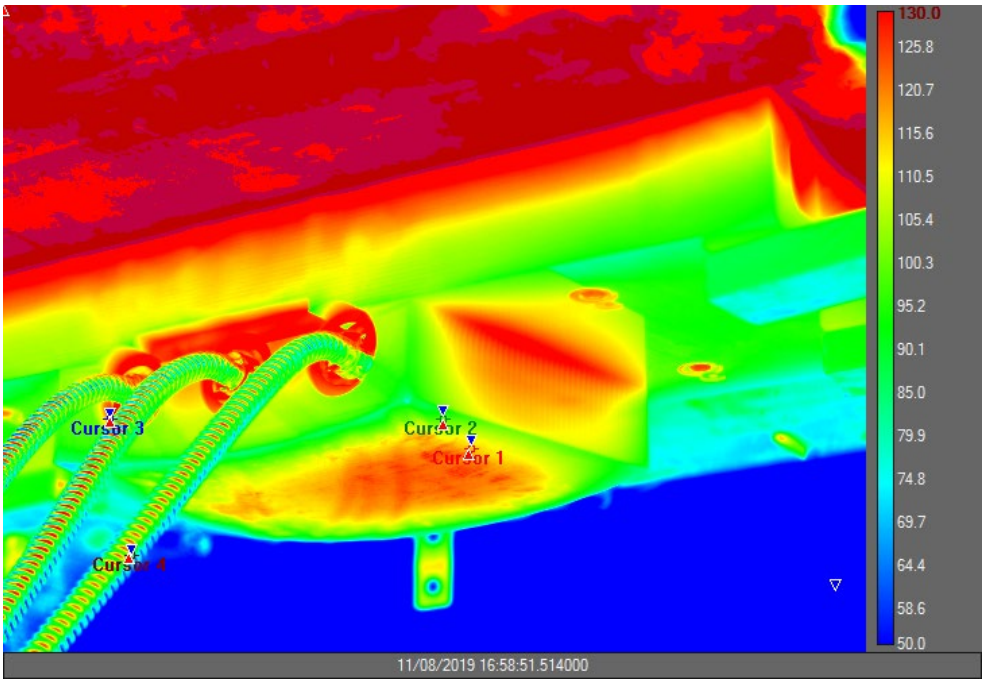

Figure 15. Temperature distribution in the positive tool before molding in °C.

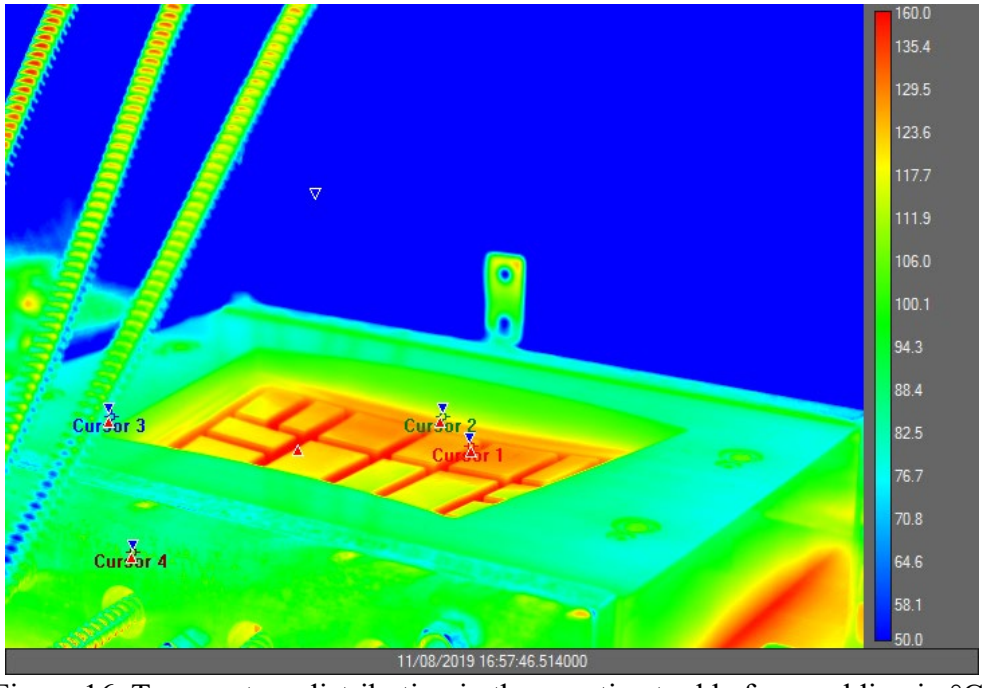

Figure 16. Temperature distribution in the negative tool before molding in °C.

A rectangular molding charge of the PPMC material with nominally 70% coverage was placed into the heated negative tool. The tool was closed for 10 sec at 10 tons (89 kN) and then the force was increased to 78 tons (694 kN) for 15 minutes. At the completion of the curing cycle, the top platen was elevated with the positive tool. When the tools separated, the part remained attached to the positive tool and was removed using hammers and chisels with manual effort. No ejector pins

were utilized in the demolding process. Figure 16 shows the consolidated part after the compression molding.

Figure 17. Successful molded part top and bottom view.

The resulting part was highly successful from visual inspection. The charge was able to fully fill the mold with limited resin push out in localized regions of the deepest ribs. This effect is a common behavior in initial molding trials, regardless of the tooling material, and can be addressed through further process optimization. The surface finish of the part shows good consolidation. Furthermore, the AM tools themselves maintained integrity after the molding. Further investigation is planned for monitoring surface deformation through multiple molding cycles.

5. CONCLUSIONS

This study has demonstrated that EDAM is a viable method to produce rapid prototype tooling for thermoset composites compression molding of moderate complexity and that simulation plays a critical role in understanding the printing process and the ultimate performance of printed parts. The LSAM process using the 25% by weight carbon fiber PESU material produced a tool that was able to maintain the molding pressures of 1500 psi (10.3 MPa) for a representative prototype production process as required to consolidate the material. While the low thermal conductivity of the polymer and composite present challenges for heating the tool, this study has demonstrated the effective utilization of internal heating strategies to achieve the required processing temperatures without negatively impacting the state of the polymer.

Modeling and simulation, utilizing the ADDITIVE3D integrated simulation workflow, drove the design of the molded part, printed tool, and the manufacturing process. The coupled thermo-mechanical simulation of the printing process provides designers with detailed understanding of how the printing strategy impacts the residual stress and deformation in the part. Furthermore, this simulation approach provides a rigorous foundation for performance models of the printed part incorporating the local, orientation dependent material properties of the composite bead in predicting behavior of the tool in the molding process. Modeling and simulation enable the part, tool, and process designers to iterate virtually, reducing the time, money, and risk associated with optimization driven by physical experimentation alone.

6. REFERENCES

[1] Sudbury TZ, Springfield R, Kunc V, Duty C. An assessment of additive manufactured molds for hand-laid fiber reinforced composites. Int J Adv Manuf Technol 2017;90:1659–64. doi:10.1007/s00170-016-9464-9.

[2] Hassen AA, Springfield R, Lindahl J, Post B, Love L, Duty C, et al. The durability of large-scale additive manufacturing composite molds. CAMX 2016 - Compos. Adv. Mater. Expo, 2016, p. 26–9.

[3] Li H, Taylor G, Bheemreddy V, Iyibilgin O, Leu M, Chandrashekhara K. Modeling and characterization of fused deposition modeling tooling for vacuum assisted resin transfer molding process. Addit Manuf 2015;7:64–72. doi:http://dx.doi.org/10.1016/j.addma.2015.02.003.

[4] Kunc V, Lindahl J, Dinwiddie R, Post B, Love L, Duty C, et al. Investigation of in-autoclave additive manufacturing composite tooling. CAMX 2016 - Compos. Adv. Mater. Expo, 2016.

[5] Barocio E, Brenken B, Favaloro A, Pipes RB. Extrusion deposition additive manufacturing of composite molds for high-temperature applications. Int. SAMPE Tech. Conf., 2017, p. 1512–23.

[6] Kuczko W, Wichniarek R, Górski F, Buń P, Zawadzki P. Application of Additively Manufactured Polymer Composite Prototypes in Foundry. Adv Sci Technol Res J 2015;9:20–7. doi:10.12913/22998624/2360.

[7] Tábi T, Kovács NK, Sajó IE, Czigány T, Hajba S, Kovács JG. Comparison of thermal, mechanical and thermomechanical properties of poly(lactic acid) injection-molded into epoxy-based Rapid Prototyped (PolyJet) and conventional steel mold. J Therm Anal Calorim 2016;123:349–61. doi:10.1007/s10973-015-4997-y.

[8] Brenken B, Barocio E, Favaloro A, Kunc V, Pipes RB. Development and validation of extrusion deposition additive manufacturing process simulations. Addit Manuf 2019;25:218–26. doi:10.1016/j.addma.2018.10.041.

[9] Brenken B. Extrusion Deposition Additive Manufacturing of Fiber Reinforced Semi-crystalline Polymers. School of Aeronautics and Astronautics, Purdue University, 2017.

[10] Barocio E, Favaloro A, Brenken B, Barocio E, Pipes RB, Favaloro A, et al. Fusion Bonding of Fiber Reinforced Semi-Crystalline Polymers in Extrusion Deposition Additive Manufacturing. School of Materials Engineering, Purdue University, 2017. doi:https://doi.org/10.1016/j.addma.2018.10.041.

[11] Favaloro AJ, Brenken B, Barocio E, Pipes RB. Simulation of Polymeric Composites Additive Manufacturing using Abaqus. Sci Age Exp 2017:103–14.

[12] Brenken B, Barocio E, Favaloro A, Kunc V, Pipes RB. Development and validation of extrusion deposition additive manufacturing process simulations. Addit Manuf 2019;25:218–26. doi:10.1016/j.addma.2018.10.041.